



HAL
open science

Understanding the mechanisms of CaO carbonation: Role of point defects in CaCO₃ by atomic-scale simulations

Rémy Besson, Loic Favergeon

► **To cite this version:**

Rémy Besson, Loic Favergeon. Understanding the mechanisms of CaO carbonation: Role of point defects in CaCO₃ by atomic-scale simulations. *Journal of Physical Chemistry C*, 2014, 118 (39), pp.22583-22591. 10.1021/jp506102c. hal-01100957

HAL Id: hal-01100957

<https://hal.science/hal-01100957>

Submitted on 7 Jan 2015

HAL is a multi-disciplinary open access archive for the deposit and dissemination of scientific research documents, whether they are published or not. The documents may come from teaching and research institutions in France or abroad, or from public or private research centers.

L'archive ouverte pluridisciplinaire **HAL**, est destinée au dépôt et à la diffusion de documents scientifiques de niveau recherche, publiés ou non, émanant des établissements d'enseignement et de recherche français ou étrangers, des laboratoires publics ou privés.

Understanding the mechanisms of CaO carbonation:
the role of point defects in CaCO₃ by atomic-scale simulations

Rémy Besson*

Groupe de Métallurgie Physique et Génie des Matériaux, Unité Matériaux et Transformations, CNRS
UMR 8207, Université de Lille 1, F-59655 Villeneuve d'Ascq, France

Loïc Favergeon

Ecole Nationale Supérieure des Mines, SPIN-EMSE, PRESSIC Department
CNRS UMR 5307, LGF, F-42023 Saint-Etienne, France

ABSTRACT

In order to improve our understanding of the mechanisms underlying the carbonation of CaO by CO₂, a practically important reaction, we present a detailed atomic-scale study, by means of ab initio density functional calculations, of the point defect properties in calcite CaCO₃. We perform a thorough investigation of the chemical potentials relevant in experimental conditions. Focusing on C and O defects closely related to CO₂ diffusion, we point out the absence of interstitial C, except possibly in complex form with other defects, whereas interstitial O is found stable. Whereas O and C vacancies are not significant in neutral form at low temperature, their role is clearly revealed when charged states are included. The formation energies of O and C vacancies, together with the profiles of chemical potentials across the growing calcite layer, are consistent with joint C and O diffusion by separate vacancy mechanisms of roughly equal amplitudes. As regards the possible influence of complex point defects, our results suggest that interstitial diffusion of CO₂ is unfavorable. Conversely, the strong binding of the CO₂ vacancy may enhance CO₂ diffusion.

Keywords: simulations, point defects, calcite, CO₂ storage

*corresponding author

INTRODUCTION

Of high practical importance is the current issue of achieving a more efficient management of carbon dioxide. This requires a better understanding of the physical mechanisms underlying the capture and release of CO₂ by suitable substrates. Among these substrates, calcium oxide CaO offers several prominent advantages [1], which turn it into a good candidate for the purpose of large numbers of capture-release cycles. The aim is to reach a better reversibility of the process, embodied in the $\text{CaO} + \text{CO}_2 \leftrightarrow \text{CaCO}_3$ carbonation reaction converting the oxide into carbonate (calcite). In the final stage of this carbonation reaction, the reaction rate is widely controlled by the diffusion of CO₂ through the carbonate layer [2], possibly via bulk as well as grain boundary mechanisms. Nothing is known about the mechanisms of CO₂ diffusion within CaCO₃, which may occur in molecular form, but also after appropriate dissociation towards O₂ or CO molecules, or even in elemental O or C species. Getting more information about CO₂ diffusion would certainly help building more realistic reaction mechanisms for the global carbonation reaction, of wide utility in macroscopic kinetic investigations [3].

On the route towards elucidating these complex questions are more basic issues connected with the point defect (PD) properties of CaCO₃, since these properties most probably have a direct influence on the CO₂ behaviour in the compound. Recently, CaCO₃ calcite has formed the subject of several atomic-scale studies, using either semi-empirical force fields or ab initio Density Functional Theory (DFT) simulations, for the modelling of bulk or surface properties [4-8] or for the investigation of nucleation from CaO [9]. As concerns PD properties, Fisler et al. [4] developed a semi-empirical shell model for CaCO₃ and applied this model to the study of PDs in this carbonate. The PDs investigated were the Ca(+2) and CO₃(-2) vacancies, and the authors also considered the Schottky pair of such vacancies. The cases of antisite defects, interstitials and other (C, O, CO₂,...) vacancies were

not studied. On the whole, the PD properties of CaCO_3 are still widely unknown, and elucidating this issue forms the subject of the present work. To this purpose, atomic-scale first-principles calculations will be employed, since the latter provide the most efficient way to probe nanoscale features hardly accessible via experiments. While CaCO_3 is a ternary compound, which makes its point defect structure rather complicated, the level of intricacy is raised further by the possibility of interstitials, and special care will therefore be given to these defects below. After describing the methodological background, the results will be presented, first in the context of neutral defects, which conveniently allows a global survey of PD properties, and then including more specifically the effect of PD charges. Our results on PDs in CaCO_3 will then be discussed in the context of CaO carbonation.

METHODS

First-principles calculations

The ab initio calculations were performed using the DFT approach, with the Vasp software [10,11] in the projector-augmented wave (PAW) framework [12] and the generalized gradient approximation (GGA) with the Perdew-Burke-Ernzerhof (PBE) [13] form of the exchange-correlation functional. A Gaussian smearing was used, together with a $4 \times 4 \times 4$ Monkhorst-Pack k-point mesh and a cutoff energy of 600 eV for the plane wave basis. All static $T=0\text{K}$ calculations included relaxations of the atomic positions as well as optimizations of the system size and shape around the PDs.

CaCO_3 calcite (Figure 1) is a rhombohedral compound ($a = 0.637 \text{ nm}$, $\alpha = 46^\circ$) containing 3 sublattices (one for each chemical species), hence 9 types of point defects (6 types of antisites, 3 types of vacancies). In addition, the possibility of single interstitial species was investigated, as described below. In the present study of PDs in calcite, most $T = 0 \text{ K}$ relaxations and all molecular dynamics calculations were performed starting from a perfect

80-atom system (supercell) containing $2 \times 2 \times 2$ $\text{Ca}_2\text{C}_2\text{O}_6$ unit cells. The effect on the PD properties of increasing the system size - up to a 270-atom supercell built on $3 \times 3 \times 3$ $\text{Ca}_2\text{C}_2\text{O}_6$ - will also be discussed.

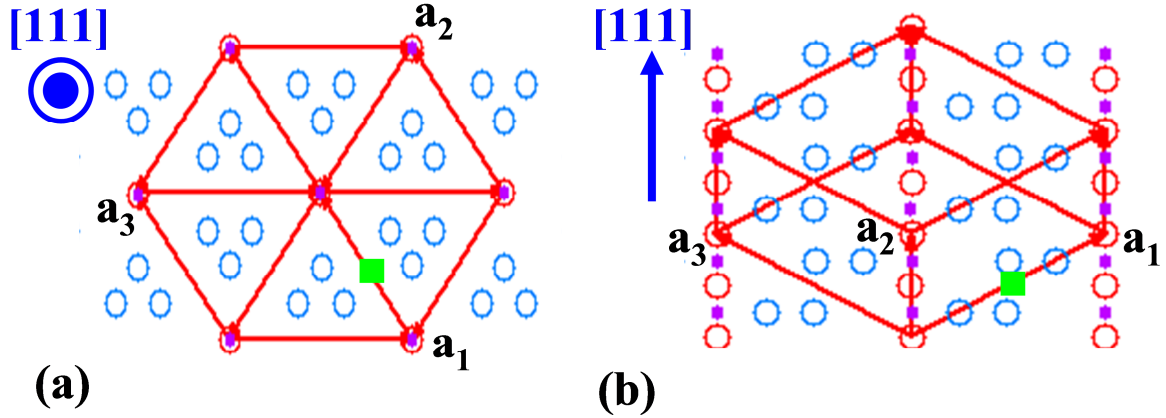


Figure 1 : Schematics of the rhombohedral unit cell ($\mathbf{a}_1, \mathbf{a}_2, \mathbf{a}_3$) of CaCO_3 calcite: (a) top view, (b) front view. The $[111]$ direction is the rhombohedral axis (third order symmetry). Ca, C and O are represented, respectively, by red circles, violine disks and blue circles. The green square depicts a $\langle 1/2; 0; 0 \rangle$ interstitial position.

IPDA modeling of point defects

Point defect-related properties in ordered compounds around stoichiometry can be conveniently investigated by means of the independent-point-defect approximation (IPDA) [14]. Initially devised for selected systems, the IPDA framework has been recently applied to various compounds with increasingly sophisticated chemistries and crystallographies. Whereas the IPDA has proved to be successful in metallic systems, including complex ordered compounds [15], its efficiency has also been demonstrated by several works on non-metallic systems involving charged defects [16-22]. These works were however mainly concerned with oxide semiconductors, and the case of carbonates such as calcite remains largely unexplored. The hypothesis underlying IPDA of independent PDs allows the energy of

the system to be written as a simple linear function of the PD amounts. Minimization of this function with respect to the PD amounts at given composition is an efficient way to obtain an overall picture of the composition-dependent PD structure of a compound at low temperature ($T = 0$ K limit) [23]. In the case of a ternary compound such as CaCO_3 , it conveniently allows to identify important composition domains characterized by two types of dominant PDs, the latter being required, even at low temperatures, to accommodate off-stoichiometry, and therefore named “constitutive” PDs. As illustrated below (section “Survey of neutral PDs”), these domains are separated by tie-lines, the crossing of which corresponds to sharp changes in the PD properties of the compound. The associated chemical potentials, which also undergo sharp changes, can be obtained easily in each domain, from the conditions of zero formation energies, in the low-T limit, for constitutive PDs together with the relations between formation energies and chemical potentials (Eq. (3) below). At higher temperatures, including various contributions to the entropy (configuration, phonons, etc.), the IPDA can be employed with either its NPT (constant particle numbers, pressure and temperature) or μVT (constant chemical potentials, volume and temperature) equivalent formulations [14], allowing to obtain the PD structure and related properties (free energy) as a function of composition and temperature, and its ability to multiple extensions towards more various fields, e.g. solution electrochemistry, has been pointed out recently [24]. The IPDA analysis relies on the determination of grand canonical (GC) energies defined, for a PD of type p and charge q , as:

$$E_{GC}(p,q) = E_{PD}(p,q) - E_{perf} \quad (1)$$

where E_{PD} and E_{perf} are respectively the total energies of defected and perfect systems of same size. It allows easy determination of the PD amounts on their respective sublattices, namely given by:

$$x(p,q) = \exp[-E_f(p,q)/kT] \quad (2)$$

where E_f is the formation energy of the PD:

$$E_t(p,q) = E_{GC}(p,q) + \delta\mu(p) + q\mu_e \quad (3)$$

where μ_e is the electronic chemical potential, controlling the global charge of the defected system. $\delta\mu(p)$ is a defect-dependent term involving the elemental chemical potentials: its value is respectively $\delta\mu(p) = +\mu(A)$ for a vacancy (V_A) on an A sublattice, $\mu(A) - \mu(B)$ for a B antisite atom (B_A) located on an A sublattice, and $-\mu(A)$ for an A atom (A_{int}) on an interstitial sublattice. Other specific temperature effects, for instance stemming from local defect-induced vibrations, can be included in relation (1) [22,25], but in the case of $CaCO_3$ this will be left for future work. Finally, it should be noted that most previous works on charged PDs were concerned with semiconductors, i.e. interested in the point defect structure in systems with possibly non-zero global charges. This explains why these works investigated the influence of the electron chemical potential, since the latter quantity controls the global charge. Conversely, in our case, although various charge states of PDs were also investigated, we did not consider the possibility of non-zero global charge. Therefore, all other (i.e. Ca, C, O) chemical potentials being determined from solid/solid and solid/gas equilibria, the electron chemical potential was obtained via Eq. (1) from the global neutrality condition.

RESULTS

Choice of chemical potentials

Table 1 : Determination of chemical potentials in $CaCO_3$: using local equilibria at the external (subscript “ext”) calcite/gas and internal (subscript “int”) calcite/oxide interfaces, relations used to obtain the elemental chemical potentials in $O_2 + CO_2$ conditions, via gaseous chemical potentials $\mu(O_2)$, $\mu(CO_2)$, and compound energies $E(CaO)$, $E(CaCO_3)$. Note that, in the present work, no attempt has been made to correlate “external” and “internal” interfaces with specific crystal planes. We simply use these words to distinguish between two different types of thermodynamic equilibria, implying different chemical potentials.

external interface (calcite/gas)	internal interface (calcite/oxide)
$\mu(\text{O}_2) = 2\mu_{\text{ext}}(\text{O})$	$\mu(\text{O}_2) = 2\mu_{\text{int}}(\text{O})$
$\mu(\text{CO}_2) = \mu_{\text{ext}}(\text{C}) + 2\mu_{\text{ext}}(\text{O})$	$E(\text{CaO}) = \mu_{\text{int}}(\text{Ca}) + \mu_{\text{int}}(\text{O})$
$E(\text{CaCO}_3) = \mu_{\text{ext}}(\text{Ca}) + \mu_{\text{ext}}(\text{C}) + 3\mu_{\text{ext}}(\text{O})$	$E(\text{CaCO}_3) = \mu_{\text{int}}(\text{Ca}) + \mu_{\text{int}}(\text{C}) + 3\mu_{\text{int}}(\text{O})$

The PD structure of an ordered compound such as CaCO_3 is well-known to depend critically on the composition, or equivalently, on the elemental chemical potentials, $\mu(\text{Ca})$, $\mu(\text{C})$ and $\mu(\text{O})$, which therefore have to be taken into account thoroughly. To this aim, it is reasonable to choose “ $\text{O}_2 + \text{CO}_2$ ” working conditions, namely characterized by a surrounding $\text{O}_2 + \text{CO}_2$ gas phase with controlled temperature and partial pressures, in order to fix $\mu(\text{Ca})$, $\mu(\text{C})$ and $\mu(\text{O})$, via $\mu(\text{O}_2)$, $\mu(\text{CO}_2)$, $E(\text{CaO})$ and $E(\text{CaCO}_3)$, according to the relations given in Table 1. In practical conditions for carbonation, a calcite layer is growing at the expense of the oxide, and the elemental chemical potentials are therefore deduced from the local equilibria existing at the external (calcite/gas) and internal (calcite/oxide) interfaces. Moreover, whereas CO_2 is active only at the external interface, it is reasonable to suppose that O_2 with uniform gaseous chemical potential exists at the internal interface as well. Under these assumptions, while $E(\text{CaO})$ and $E(\text{CaCO}_3)$ are directly obtained from ab initio calculations of solid compounds, the gaseous chemical potentials $\mu(\text{O}_2)$ and $\mu(\text{CO}_2)$ can be conveniently obtained from statistical thermodynamics descriptions of ideal gases, using ab initio estimations of energies for isolated O_2 and CO_2 molecules, together with rotation and vibration partition functions obtained using characteristic frequencies from experiments available in literature. Resorting to literature data for the vibration and rotation parts avoids

performing ab initio calculations for these quantities, which is justified by previous studies [26] on CO₂ demonstrating the excellent agreement between DFT calculations and literature data. Moreover, it was previously found [27] that efficient experimental conditions for the carbonation reaction correspond to CO₂ pressures ranging between 2 and 30 kPa, while the O₂ pressure is maintained at low values, typically 100 Pa.

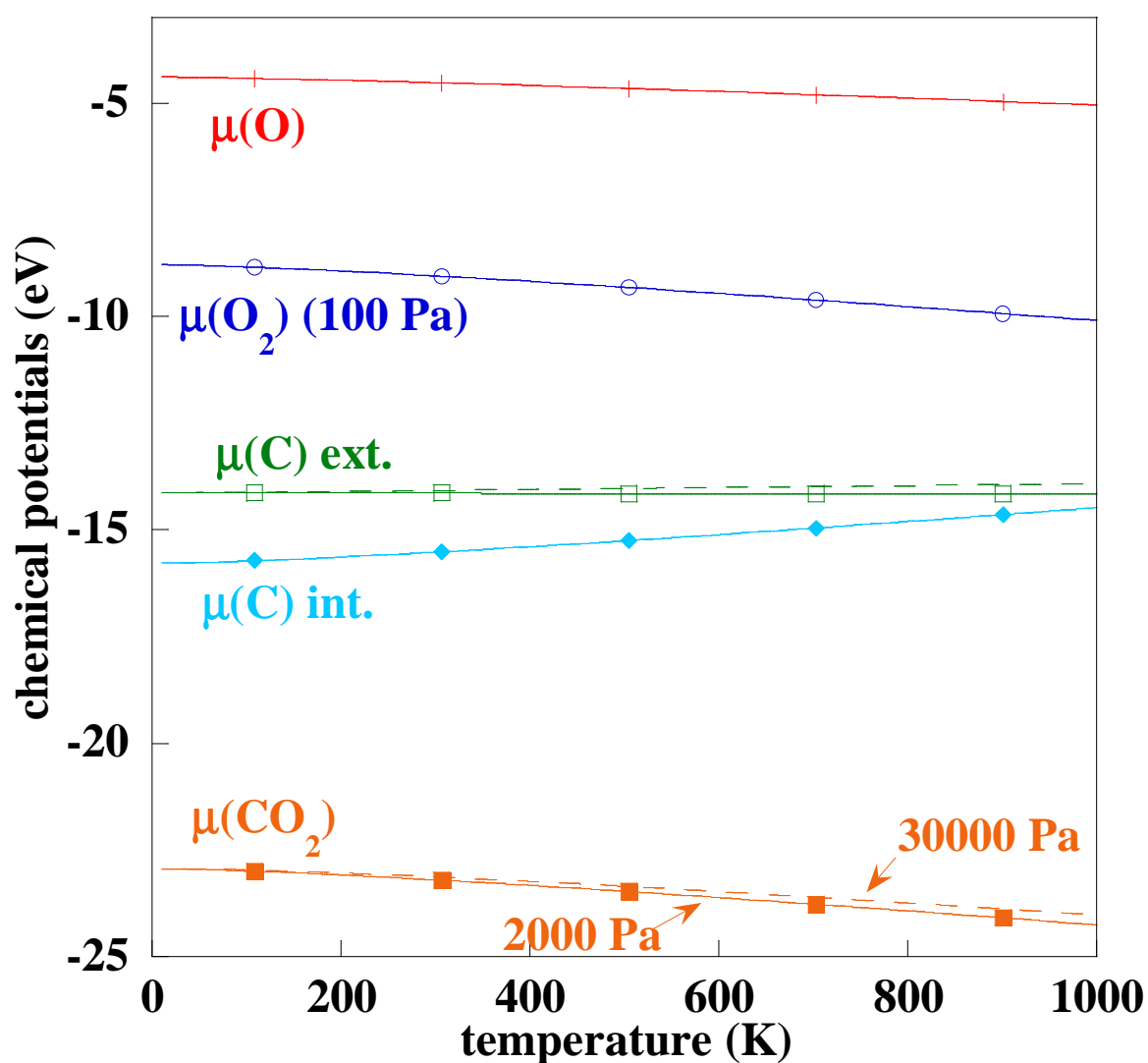


Figure 2 : From ab initio-based calculations, chemical potentials of gaseous O₂ and CO₂ molecules as a function of temperature, together with the corresponding elemental chemical potentials of C and O at the external (calcite/gas) and internal (calcite/oxide) interfaces. While

$P(\text{O}_2) = 100$ Pa throughout, the effect of $P(\text{CO}_2)$ is investigated (full lines: 2000 Pa, dashed lines: 30000 Pa).

Using these conditions, the effect of temperature on the gaseous and elemental chemical potentials is displayed on Figure 2. These previous experiments [27] suggested using 800 K as working temperature, and the latter will thus be considered in our work. At this temperature, while the pressure effect on $\mu(\text{CO}_2)$ appears rather low in the range of interest, the local equilibria imply that the C chemical potential is significantly lower (~ 1 eV) at the internal interface than at the external one. Finally, it is important to note that, while $\text{O}_2 + \text{CO}_2$ conditions were selected as most convenient for our theoretical study, they will have to be compared (see Discussion below) with available experimental results, obtained under $\text{H}_2\text{O} + \text{CO}_2$ conditions often used in practice. Indeed, the oxygen residual pressure is often overlooked in experiments, contrary to $P(\text{H}_2\text{O})$, which was shown to have a critical effect on the carbonation rate [28].

Interstitial defects in CaCO_3

Due to the low symmetry of the CaCO_3 structure, finding the possible sites occupied by interstitials species is an intricate issue. To this purpose, ab initio molecular dynamics was employed to investigate the properties of interstitials in CaCO_3 . As a first step, using the three equivalent positions $\langle 1/2; 0; 0 \rangle$ (top part of Figure 3) as a reasonable starting point, systems containing each interstitial species on this position were initially relaxed to $T = 0$ K and zero pressure. In a second step, each system was then submitted to 2000 steps (1 fs) of molecular dynamics, using a 1000 K initial temperature and NVE conditions, namely with constant particle numbers, volume and energy. Figure 3 (bottom part) displays the final configuration for each species. As a main result, the interstitial behaviour appears to be strongly species-dependent. Interstitial Ca undergoes an instability, which spontaneously converts it into a

$\text{Ca}_\text{C} + \text{C}_\text{int}$ two-site complex PD (Figure 3a). Likewise, isolated interstitial C is unstable, and produces a three-site $2\text{C}_\text{int} + \text{V}_\text{C}$ complex (Figure 3b). Conversely, interstitial O is found to be stable (Figure 3c). On the whole, O will therefore be the only species considered as possibly occurring in simple interstitial form in CaCO_3 . We will briefly discuss the possible effect of complexes, such as the previous ones, including C_int . Such complexes, however, should be hardly mobile, having thus no influence on the diffusion properties in calcite.

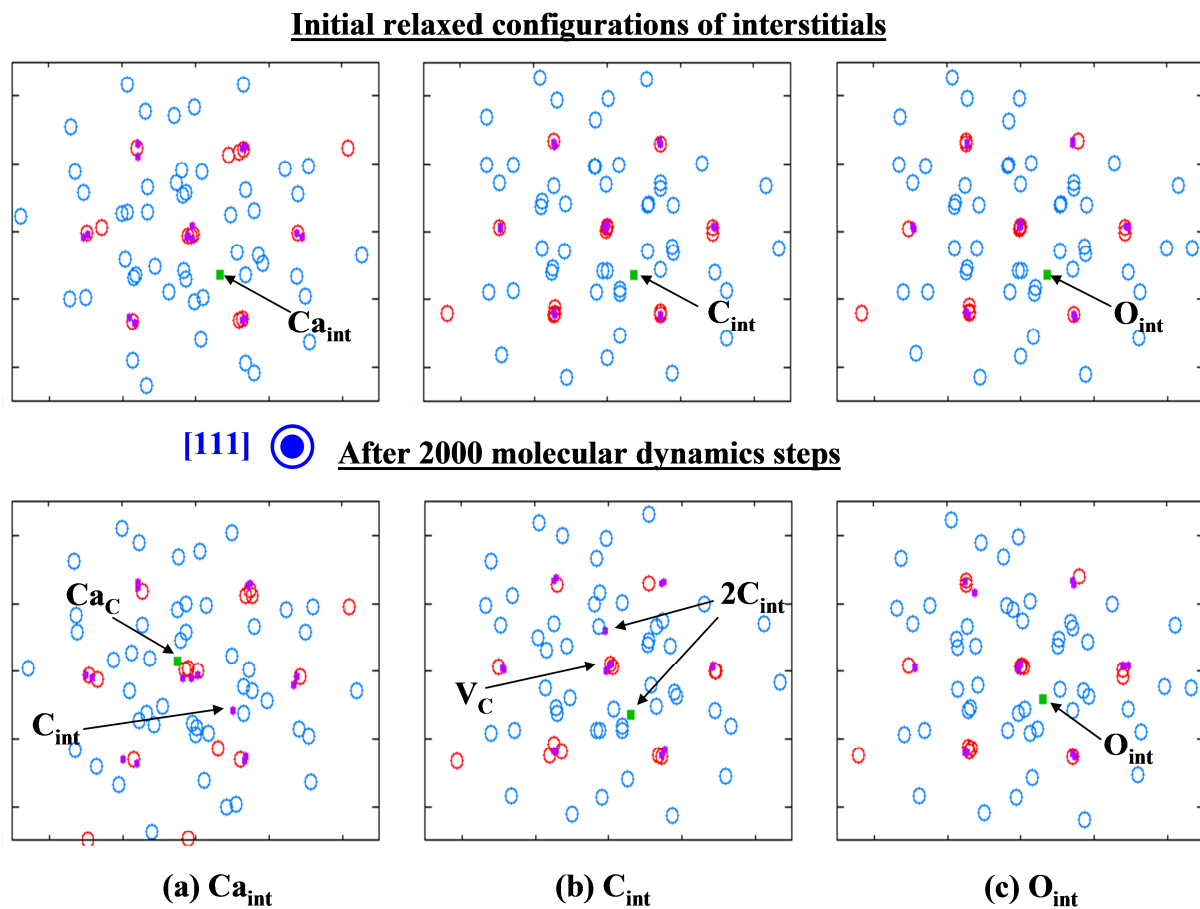


Figure 3 (color online) : Behaviour of interstitial defects in calcite viewed along the [111] direction: initial relaxed positions of interstitials (top pictures), and configurations after 2000 steps of ab initio molecular dynamics for the various chemical species: (a) Ca, (b) C and (c) O interstitials (DFT calculations in the PAW-PBE framework). The interstitials are added to an 80-atom reference system built from $2 \times 2 \times 2$ $\text{Ca}_2\text{C}_2\text{O}_6$ unit cells. The symbols of chemical species are the same as on Figure 1.

Survey of neutral PDs

Due to the complexity of the CaCO_3 structure, involving a priori 9 types of PDs as well as O interstitials, it is useful, in a first step, to confine our investigations to neutral defects and low temperature. The main advantage of this preliminary study is to provide an easy “at-a-glance” picture of the PD properties of the compound. On the other hand, including temperature and charges (next section) makes the analysis more cumbersome, which imposes to focus on selected working conditions (such as those described above) and fails in yielding a comprehensive idea of the PD properties of the compound.

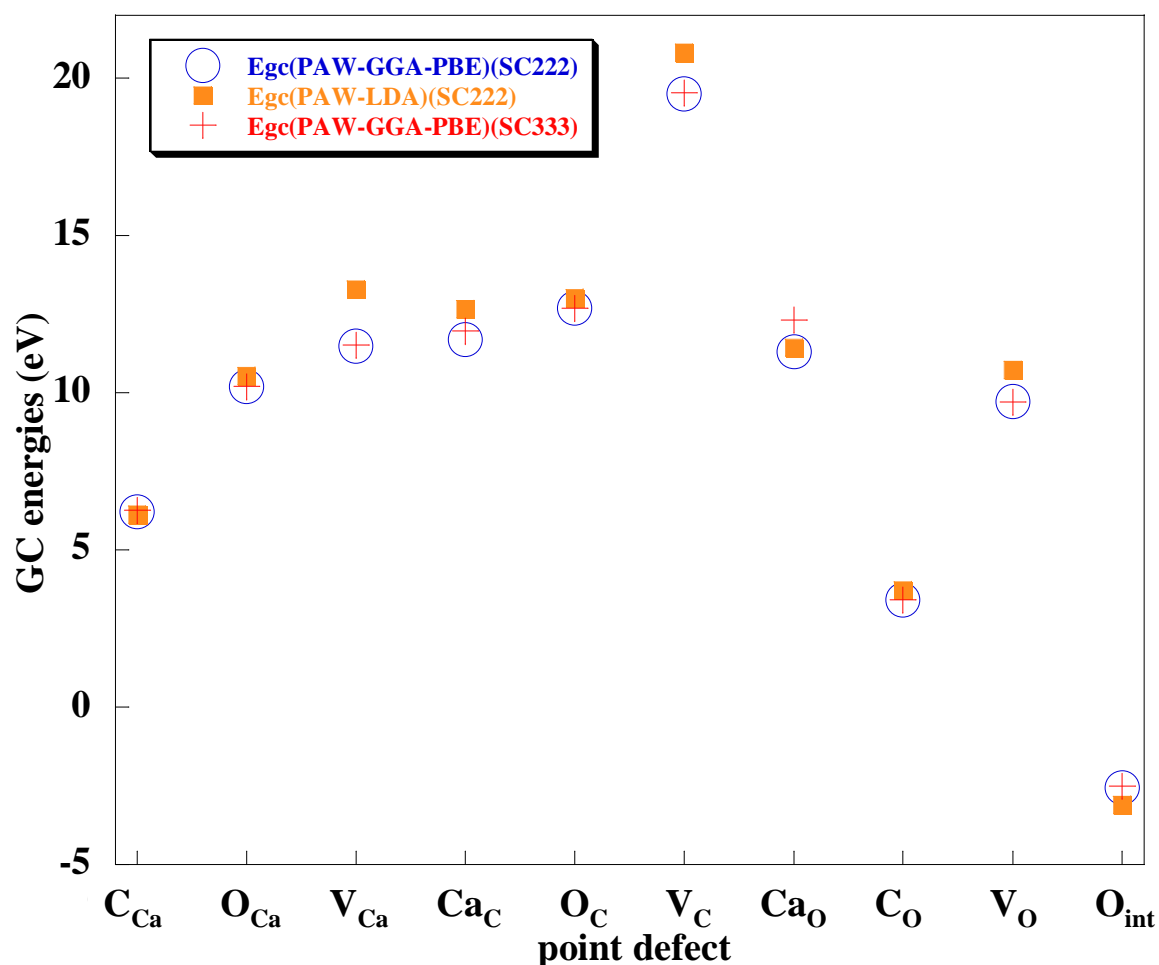


Figure 4 : Grand canonical energies of neutral point defects in CaCO_3 , in $2 \times 2 \times 2$ $\text{Ca}_2\text{C}_2\text{O}_6$ unit cells from PAW-PBE (circles) or PAW-LDA calculations (squares), and in $3 \times 3 \times 3$ $\text{Ca}_2\text{C}_2\text{O}_6$ systems for PAW-PBE (crosses).

Following these lines, the PAW-PBE grand canonical energies of neutral PDs are displayed on Figure 4 in the case of $2 \times 2 \times 2$ systems (empty circles) for all relevant PDs, namely excluding interstitial Ca and C due to their instability pointed out in the previous section. Figure 4 also displays the GC energies obtained for $3 \times 3 \times 3$ systems (crosses), showing excellent convergence except for Ca_0 . For purpose of comparison, PAW-LDA results are also presented (full squares). Although global trends are the same as for GGA, some dispersion however exists, especially for Ca and C vacancies, which suggests that further investigation would be useful in precisising the effect of the choice of the DFT scheme on the PD and diffusion properties of CaCO_3 . In this work, however, we will confine to the PAW-PBE framework, leaving such investigation for future.

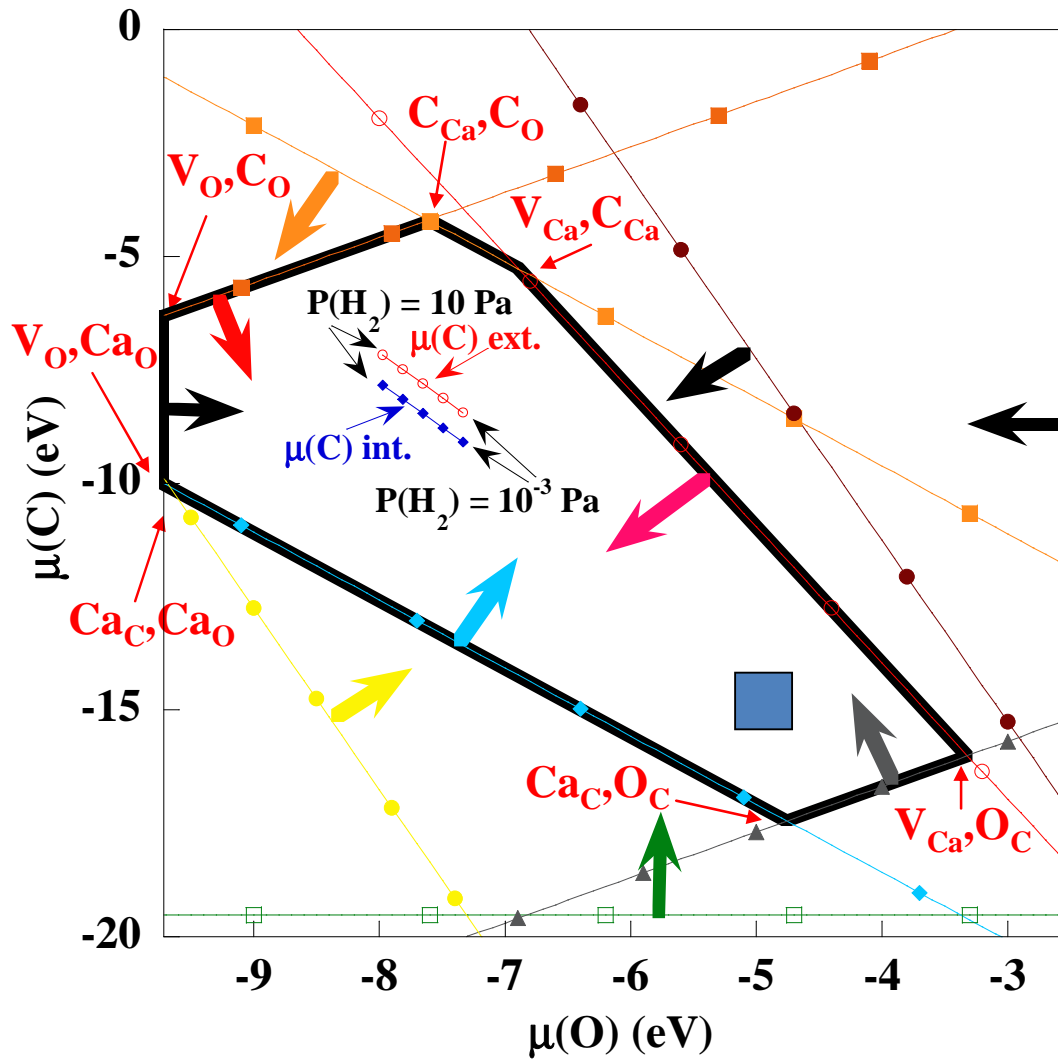


Figure 5 : Validity domain (area surrounded by bold line segments) of O and C chemical potentials, as obtained from positivity conditions for all formation energies of neutral PDs (one line for each PD, the arrow indicates the half-plane respecting this condition – various colors are used as a guide for the eye). Each corner of the domain corresponds to the $T = 0$ K $\mu(\text{O})$ and $\mu(\text{C})$ values given on Figure 6 (PAW-PBE calculations). The blue and red straight lines within the validity domain will be discussed below (“Discussion” part). The blue square indicates the working conditions of Fig. 2.

While the elemental chemical potentials, i.e. $\mu(\text{C}) \sim -15$ eV and $\mu(\text{O}) \sim -5$ eV, relevant for experimental conditions of calcite formation are given on Figure 2, it is instructive to

confront these values with their counterparts deduced from the PD properties of calcite, since the chemical potentials of ordered compounds are known to be strongly sensitive to temperature and composition around stoichiometry. The present low-temperature survey of PD properties easily allows to estimate the consistency between (i) the above choice of $\mu(\text{C})$ and $\mu(\text{O})$ from gaseous conditions and (ii) the chemical potentials deduced from the CaCO_3 compound properties. Noticeably, this provides a way to investigate the validity and transferability (gas vs solid) of the ab initio DFT framework used for. To this aim, since all the PD formation energies defined by relation (1) have to be positive, this provides conditions on the elemental chemical potentials, which implies that these quantities have to be confined to a restrictive domain. This is described on Figure 5, which displays this domain as a polygon, each corner of which corresponding to a composition domain (see Figure 6 below) characterized by a couple of structural PDs. Conversely, each polygon edge corresponds to a (infinitely at 0 K, see Figure 6) thin line of transition between a defect type and a neighbouring one. In this context, the working conditions deduced from Figure 2 are depicted as a blue square on Fig. 5, which indicates that, although these conditions are located on an edge of the positivity domain, $\mu(\text{C})$ and $\mu(\text{O})$ can be varied of a few eV within this domain. However, a strong lowering of $\mu(\text{O})$ should be compensated by an increase in $\mu(\text{C})$, which will be illustrated below (“Discussion” part) when discussing $\text{H}_2\text{O} + \text{CO}_2$ conditions. On the whole, Figure 5 confirms the ability of the selected PAW-PBE framework to describe the gaseous as well as the solid properties relevant for the $\text{CaO} + \text{CO}_2 \leftrightarrow \text{CaCO}_3$ reaction.

Following the IPDA framework, the E_{GC} parameters straightforwardly provide a survey of the composition-dependent PD structure of CaCO_3 at low temperature. The $T = 0$ K limit allows to emphasize only the major “structural” defects, required to accommodate for departures from stoichiometry, while discarding other, thermally activated types of PDs. The results, displayed on Figure 6 in a form similar to representations of ternary phase diagrams,

evidence seven domains delimited by various composition tie-lines (x_{Ca} , x_C and x_O being the atomic fractions in the compound, $x_{Ca} + x_C + x_O = 1$), namely a rather intricate PD structure for the $CaCO_3$ compound. Providing the composition-dependent counterpart of Figure 5 (associated with chemical potential-dependent properties), this demonstrates the sensitivity of $CaCO_3$ to the external conditions, such as the gaseous surrounding, and the influence of these conditions on the $CaCO_3$ composition and PD-based properties, especially diffusion. As main predicted properties for PDs in calcite, C vacancies and interstitial O are never found as major defects whatever the composition range. Conversely, various types of antisites do occur, and O or Ca vacancies may be favoured depending on the composition domain. Corresponding to these PDs, the analysis also yields the chemical potentials of the $CaCO_3$ ordered phase, constant in each composition domain in the low-temperature limit (Figure 6, also each polygon edge on Figure 5). Confronting these results with the chemical potentials deduced from the gas phase allows to connect the relevant PD domains with the composition range of the compound in working conditions. This range is embodied by the arrows represented on Figure 6, suggesting the importance of the $x_{Ca}=1/5$ tie-line, and to a secondary extent that of $x_O=3/5$ and $x_O=3x_C$. In this relevant composition domain, the carbonate should be characterized by Ca vacancies together with Ca_C and O_C antisites. Whereas these major PDs are probably consistent with Ca diffusion, they do not provide any easy explanation for the diffusion of elemental O and C, while this should be of primary importance in case of dissociation of the CO_2 molecule at the external interface. This may indicate that CO_2 diffuses as such within the layer, a hypothesis to be examined further (see below). Moreover, our results suggest that the domains of variation of chemical potentials, when going from the external to the internal interface, may lead to the crossing of the $x_{Ca}=1/5$ line, hence a possible change of the PD structure across the carbonate layer. This probably implies a change of the

diffusion properties, especially for Ca, but this is not critical for carbonation, since this reaction is not submitted to Ca diffusion.

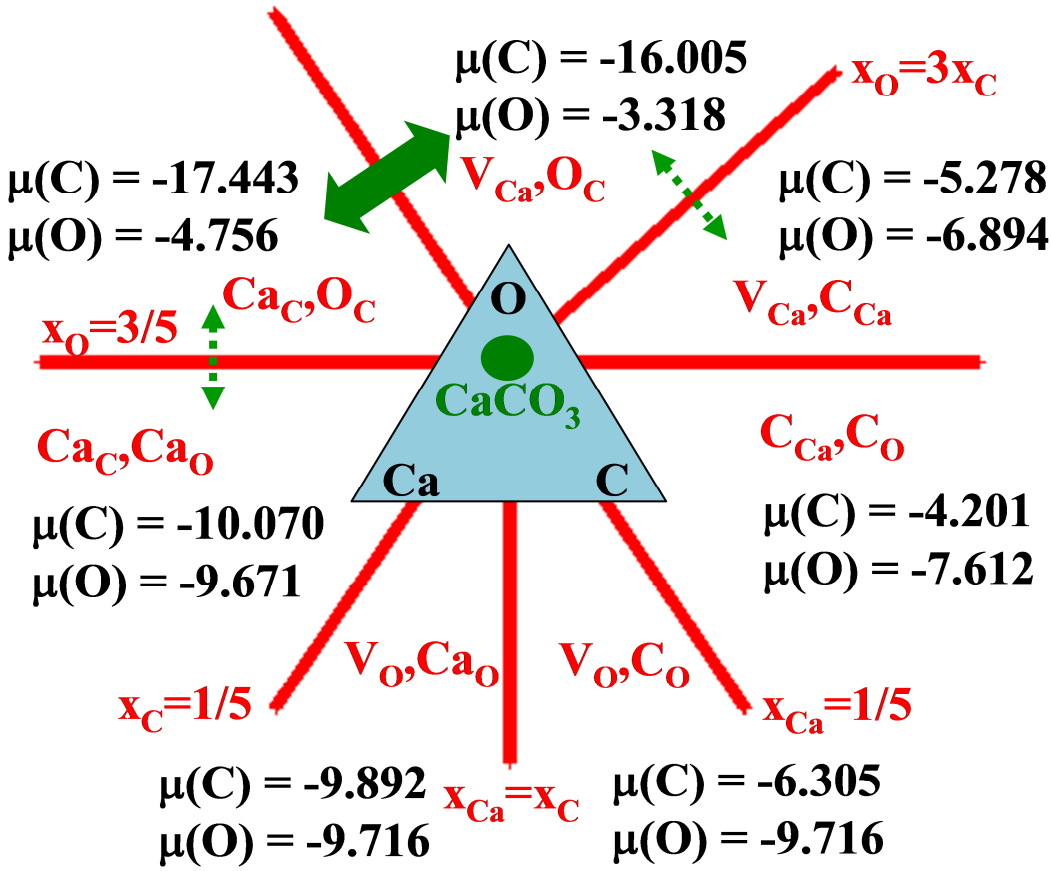


Figure 6 : Survey of composition-dependent structure of neutral point defects of CaCO_3 in the $T = 0 \text{ K}$ limit, as obtained from grand canonical energies in $2 \times 2 \times 2 \text{ Ca}_2\text{C}_2\text{O}_6$ unit cells and PAW-PBE framework. The central triangle figures out the ternary phase diagram representation of compositions around stoichiometric CaCO_3 (central full circle). In each composition domain, the O and C chemical potentials (eV units) are displayed, as deduced from the IPDA analysis. The arrows indicate likely domains of stability for the compound, according to the elemental chemical potentials deduced from Table 1 and Figure 2.

Charged defects

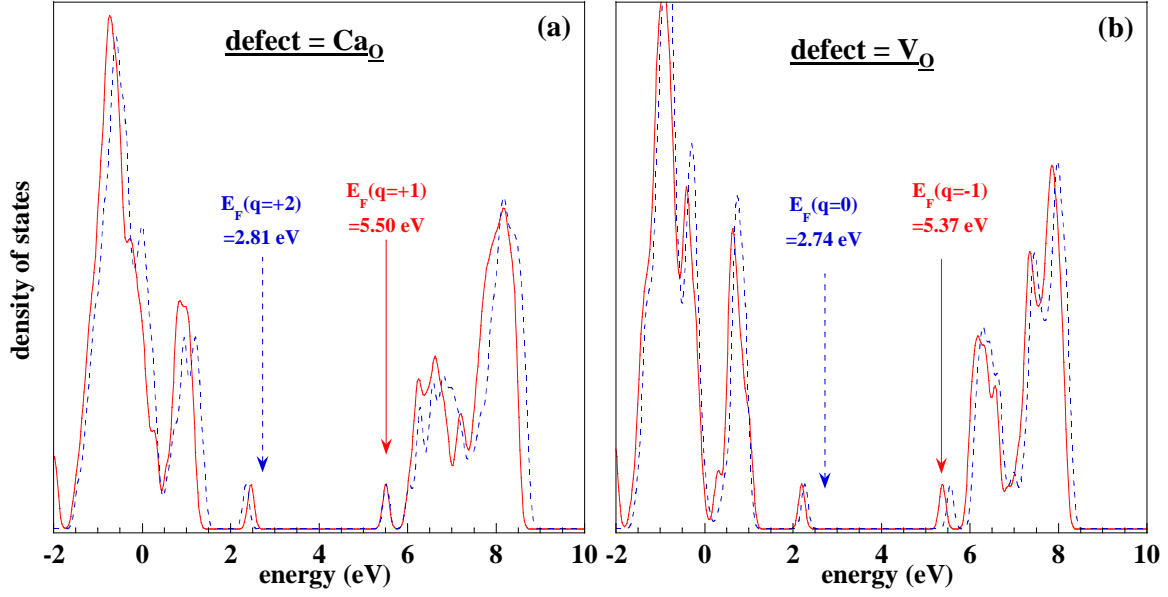


Figure 7 : Electronic densities of states for charged defects in calcite: (a) Ca_O (q=+1/+2) and (b) V_O (q=-1/0) (PAW-PBE calculations in 2x2x2 systems).

While the previous study allowed to describe the main trends of PDs in CaCO₃, it was restricted to neutral PDs, whereas the presence of charged defects may be possible in such carbonates. Investigating charged PDs requires the knowledge of the electronic densities of states (DOSs), primarily for the perfect, undefected system, since it directly influences the amounts of conduction electrons and valence holes, hence the global charge balance. In addition, the DOS for each type of charged PD is valuable as it may provide information about defect instabilities possibly occurring for specific charge levels. Although such instabilities have hitherto been reported in some semiconductors like Ga₂O₃ [22], similar features cannot a priori be discarded in carbonates. To clarify this issue for CaCO₃, all charge levels in the range $\{-2 ; +2\}$ were taken into account for all PDs, this range being possibly extended up to $q = +/-4$ for some defects, when this was required to localize the formation energy minimum according to relation (1). From inspection of all corresponding DOSs, the most remarkable result is obtained in the cases of Ca_O for $q < +2$ (Figure 7a) and V_O for $q < 0$

(Figure 7b): whereas in most cases the Fermi level is located within, or closely above, the valence band, such charged defects correspond to additional peaks of occupied states just below the conduction band. As will be checked below by the detailed analysis of formation energies, this should entail a strong increase of energy cost for these charge levels, and the latter should thus be unstable. For all other PDs and charges, the DOSs (not shown for brevity) sometimes reveal the existence of intermediate peaks located in the gap, especially for C_{Ca} , O_C , C_O and O_{int} , but contrary to Ca_O and V_O , the analysis below will indicate no such charge-dependent changes of behaviour for these PDs.

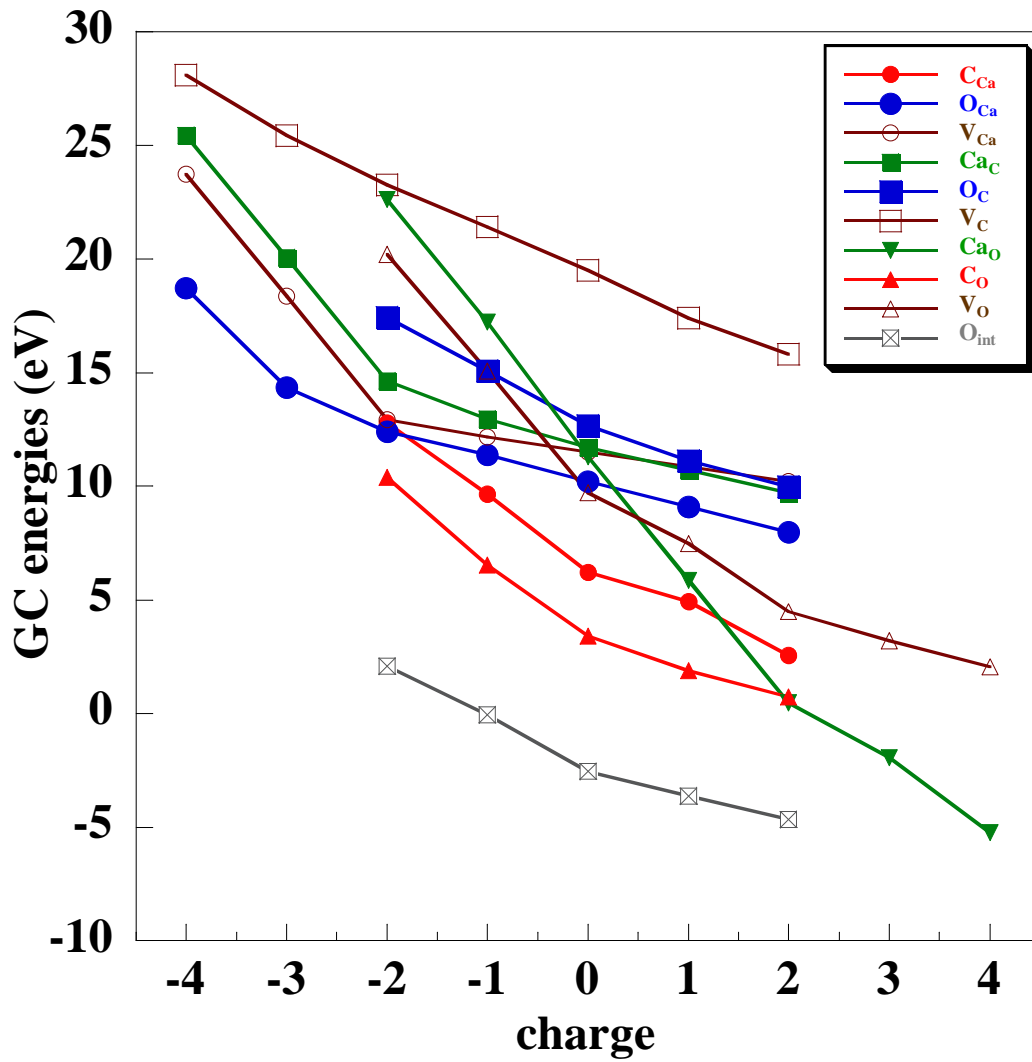


Figure 8 : GC energies of charged defects in calcite, from ab initio PAW-PBE calculations (2x2x2 systems).

The GC energies of charged defects, displayed on Figure 8, show a globally increasing trend with charge decrease. This suggests that the dominant effect is due to the band energy, a more negative charge entailing the occupation of higher one-electron energy levels in the DFT framework. The other contributions to the total energy are not sufficient to modify this globally monotonic behaviour. For charges comprised between -2 and +2, the slope is quite identical for all PDs, except for Ca_O and V_O, namely both PDs pointed out in the previous DOS analysis. A similar behaviour is detected for V_{Ca} and Ca_C, though for more negative

charges. These GC energies allow to investigate the formation energies of charged defects in $O_2 + CO_2$ working conditions (Figure 9). In these conditions, $CaCO_3$ is found to be exactly stoichiometric (to within 10^{-4}) and $\mu_e = 1.432$ eV for charge neutrality. Considering Ca defects, V_{Ca} is found to be strongly stabilized by $q = -2$, whereas values $= -2$ and $> +2$ are required for Ca_C and Ca_O respectively. With a formation energy of ~ 0.5 eV, the Ca vacancy remains by far the most stable PD in $CaCO_3$, which is consistent with our previous results obtained from neutral defect analysis, pointing out V_{Ca} as structural defect. This conclusion is not ruled out by charge effects. As for C defects, C_{Ca} and C_O have very similar behaviours, being more stable in neutral state, but their energies remain very high. Conversely, V_C displays a much lower formation energy (~ 3 eV) and a moderate charge dependence, which should probably turn it into a favourable defect in various conditions. Finally, as regards O defects, V_O remains neutral in its most favourable state ($E_f \sim 4$ eV), while O_C and O_{int} have very close formation energies (~ 3 eV) and may adopt competing charge levels between -2 and 0, and O_{Ca} requires $q = -3$ though maintaining a high formation energy (~ 5 eV). Finally, it is worth noting that V_O , V_C and O_{int} have relatively low formation energies, which makes them good candidates for C and O diffusion in the context of CaO carbonation.

DISCUSSION

Our results on PDs in calcite can be compared with those of previous works, in particular the semi-empirical shell model for $CaCO_3$ proposed by Fisler et al. [4]. The only comparison with our work is possible for $V_{Ca(+2)}$ with a formation energy of ~ 20 eV, to be compared with ~ 7 eV in our work for the same charge level. Although the difference is quite large, both works agree to indicate that positively charged Ca vacancies are energetically unfavourable, and our work, considering other charge levels for this defects, indicates that a negative charge is more favourable. Moreover, both works differ in the chemical potentials

selected in order to obtain the formation energies (Eq. (3) in our work), which may explain the numerical discrepancy for $V_{\text{Ca}(+2)}$. More systematic investigations would be required to compare the semi-empirical and ab initio energetics of CaCO_3 .

The previous results were obtained for PDs periodically repeated in $2 \times 2 \times 2$ unit cells of $\text{Ca}_2\text{C}_2\text{O}_6$, which raises the issue of possible interactions between defects. While Figure 4 indicates that such interactions can reasonably be neglected for neutral systems, the case of charged defects may require further investigation, due to the long-range nature of electrostatic energies. For larger systems consisting of $3 \times 3 \times 3$ unit cells, each given (PD ; charge) involves ~ 270 atoms, which remains very demanding for current computational resources. Since the wide panel (~ 60) of PD types and charges in calcite leads to exceedingly long calculations, we therefore limited our study of these intricate convergence issues to several cases of PDs. In these cases, we checked that our PD analysis using $2 \times 2 \times 2$ unit cells led to errors $< 10\%$ in GC energies, which is reasonable in regard of the other possible sources of uncertainties inherent to the ab initio – IPDA approach, e.g. the validity of the PAW-PBE energy model. We thus leave more accurate investigations for future works. Finally, the issue related to the alignment of local electrostatic potentials, also connected with the handling of charged systems [16], was also examined for PDs in CaCO_3 , but the possible offsets (< 0.5 eV) were not found significant with respect to other sources of errors.

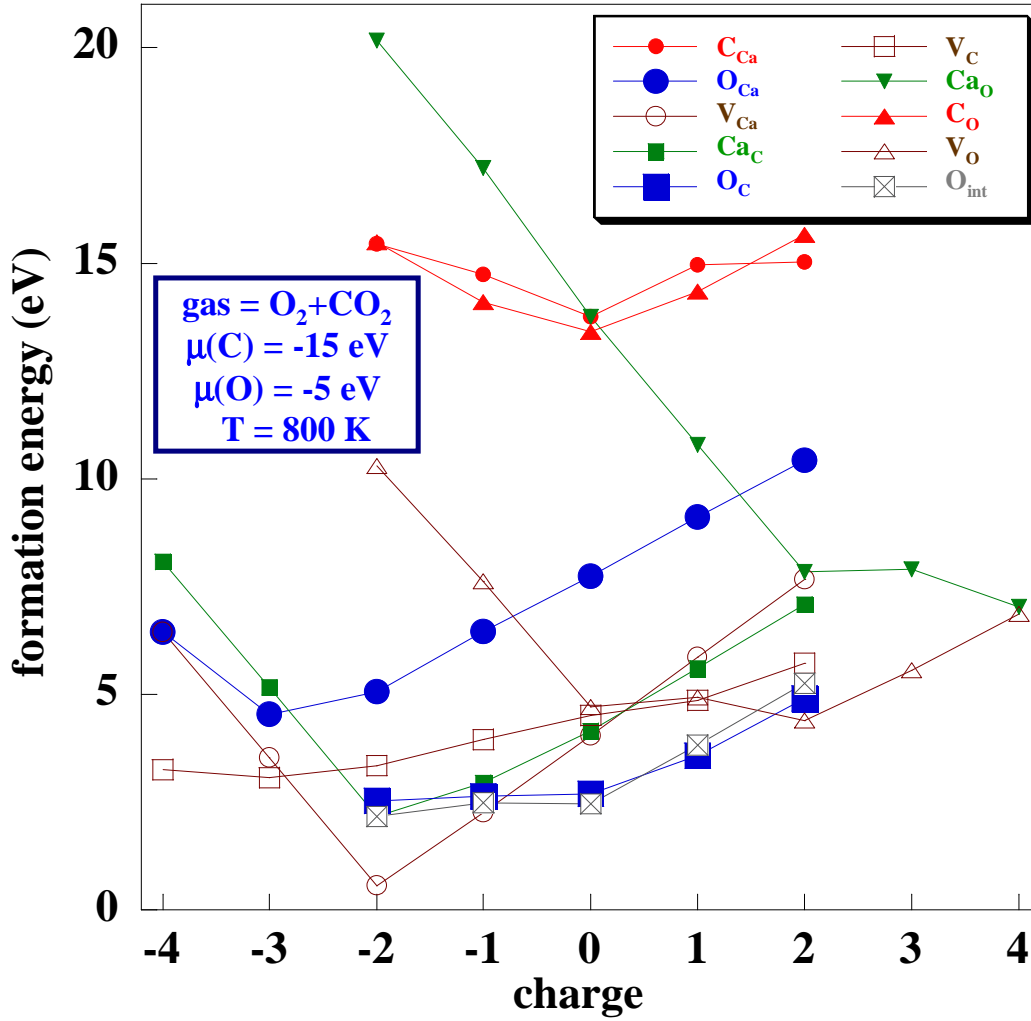


Figure 9 : Formation energies of charged and neutral defects in $CaCO_3$ under “ O_2+CO_2 ” (see text) working conditions: $T = 800$ K, $\mu(C) = -15$ eV, $\mu(O) = -5$ eV, from ab initio PAW-PBE calculations.

Our study of point defects in calcite, emphasizing the roles of O and C vacancies, suggests that C and O diffusion in $CaCO_3$ may occur by vacancy mechanisms. Moreover, it is worth noticing that the profiles of C chemical potentials across the calcite layer imply (using relation (1) and $\mu(C)_{int.} < \mu(C)_{ext.}$ on Figure 2) that the V_C formation energy should be lower at the internal interface. This entails a higher concentration of V_C , hence a V_C flux towards the external interface, namely an opposite flux of C atoms towards the internal

interface, which is the zone where carbonation occurs. The existence of such gradients for C will also be shown to be true in $\text{H}_2\text{O} + \text{CO}_2$ conditions, see Table 2. Although the same argument cannot be applied to O vacancies under our hypothesis of equal O chemical potential at both interfaces, a driving force for the ext. \rightarrow int. O flux may stem from a strong binding between C and O vacancies, as seen below.

Table 2 : In $\text{H}_2\text{O} + \text{CO}_2$ conditions ($P(\text{H}_2\text{O}) = 200 \text{ Pa}$, $P(\text{CO}_2) = 2000 \text{ Pa}$) and for $T = 800 \text{ K}$, influence of H_2 pressure (Pa) on the H_2 , O and C chemical potentials (eV) at the internal and external interfaces.

H_2 pressure	$\mu(\text{H}_2)$	$\mu(\text{O})(\text{ext/int})$	$\mu(\text{C})(\text{ext})$	$\mu(\text{C})(\text{int})$
10^{-3}	-7.73	-7.35	-9.22	-9.88
10^{-1}	-7.41	-7.67	-8.59	-9.24
10	-7.09	-7.98	-7.95	-8.61

While the previous low-T analysis suggested that both the $x_{\text{Ca}} = 1/5$ and $x_{\text{O}} = 3x_{\text{C}}$ tie-lines may be important in determining the PD properties of calcite, the more precise account of $\text{O}_2 + \text{CO}_2$ working conditions performed in this section allows to focus on the role of $x_{\text{O}} = 3x_{\text{C}}$. Crossing this tie-line may imply deep changes in thermal defects within the calcite layer. In order to explore this possibility, we have checked that small changes of $\mu(\text{C})$ entail no change of PD type across the calcite layer.

While this work was mainly focused on simple PDs in calcite, our preliminary study of interstitials, stressing Ca and C instabilities, also reveals the formation of complex defects, namely $2\text{C}_{\text{int}} + \text{V}_{\text{C}}$ and $\text{Ca}_{\text{C}} + \text{C}_{\text{int}}$. In the context of CaO carbonation by carbon dioxide, it therefore seems reasonable to consider possible connections between complex PDs and CO_2

diffusion in calcite. Although a detailed investigation of complex defects in CaCO_3 is beyond the scope of this work, two complexes come to mind naturally in this framework, namely CO_2 (i) vacancy and (ii) interstitial. As for the latter case, our investigations suggest that interstitial C should be accompanied by C vacancies, rather than by interstitial O as required in the CO_2 molecule. Confirming this point would imply additional molecular dynamics investigations, in order to attempt to detect possible favourable sites for the CO_2 molecule within the calcite lattice. Leaving this highly exploratory task for future work, we here emphasize the role of the CO_2 vacancy located in a CO_3 plane of CaCO_3 , for which ab initio calculations indicate a strong binding energy ~ 11.6 eV in neutral form. Comparing this value with the formation energies of the isolated corresponding neutral defects (Figure 9) leads to a CO_2 vacancy formation energy below 1 eV, a remarkably low value for such a complex PD, which should entail a strong enhancement of CO_2 diffusion via the complexation of O and C vacancies. Further insight into this issue would be gained from investigating the diffusion mechanisms in the calcite structure.

Table 3 : Comparison of PD formation energies (eV) in $\text{O}_2 + \text{CO}_2$ and $\text{H}_2\text{O} + \text{CO}_2$ working conditions. The most stable charge level, indicated between parentheses, was selected for each defect (for $\mu(\text{C})$ at external interface). Values relative to PD relevant for diffusion during carbonation are highlighted.

defect	$\text{O}_2 + \text{CO}_2$	$\text{H}_2\text{O} + \text{CO}_2$	
		$\text{P}(\text{H}_2) = 10^{-3} \text{ Pa}$	$\text{P}(\text{H}_2) = 10 \text{ Pa}$
$\text{V}_{\text{Ca}}(-2)$	0.57	1.0	1.2
$\text{C}_{\text{Ca}}(0)$	13.8	9.3	8.6
$\text{O}_{\text{Ca}}(-3)$	4.5	6.9	8.7

V_C(-3)	3.1	7.4	7.8
Ca _C (-2)	2.2	5.8	6.0
O _C (-2)	2.5	9.8	11.3
V_O(0)	4.4	2.4	1.7
Ca _O (+4)	7.0	5.1	4.2
C _O (0)	13.4	5.3	3.4
O_{int}(-2)	2.2	3.7	3.9

As mentioned in the introduction, it is also useful to consider CO₂ + H₂O working conditions, which correspond to carbonation performed under controlled water, rather than oxygen, pressure. These conditions are important in practice [28], previous works indicating gas pressures P(H₂O) = 200 Pa and P(CO₂) = 2000 Pa as efficient for CaO carbonation. The O chemical potential $\mu(O)$ is determined via the dissociation equilibrium of H₂O, which however leaves the H chemical potential undetermined. In the present work, the latter was therefore considered as a parameter controlled by H₂ gas. To elucidate the influence of this parameter, we studied (Table 2 and thin lines on Figure 5) the variation of $\mu(C)$ and $\mu(O)$ with $\mu(H_2)$ at 800 K and (P(H₂O) = 200 Pa, P(CO₂) = 2000 Pa). From these data, Table 3 then displays the comparison of PD formation energies in O₂ + CO₂ and H₂O + CO₂ working conditions with $\mu(C)$ at the external interface. It shows that the choice of conditions has a strong influence on the PDs. In particular, while V_{Ca} remains dominant in both cases, V_C and V_O are strongly affected by O₂ vs H₂O control: whereas the former case corresponds to relatively equal amounts of these defects, the latter deeply breaks the balance in favour of V_O while also raising the role of O_{int}. The efficiency of purely vacancy mechanisms for joint O and C diffusion should thus be lowered in H₂O + CO₂ conditions, the diffusion of O occurring

then by interstitial mechanism. Moreover, the $P(\text{H}_2)$ influence remains quite moderate, which suggests that our conclusions are reliable whatever the experimental conditions for which this parameter remains uncontrolled.

Finally, it is useful to emphasize the connection between our work, providing clear-cut trends on point defect properties in CaCO_3 , and the more general context of CaO carbonation by carbon dioxide. The carbonation reaction, which occurs at the internal CaO/CaCO_3 interface, requires diffusion of O and C through the carbonate layer. Since diffusion is mediated by point defects, the present atomic-scale results on point defects in CaCO_3 provide a first, but necessary, step towards this connection. Our work gives hints on how to select those relevant species for diffusion: it indicates that such species could reasonably include O and C vacancies, as well as interstitial O (but not interstitial C) and CO_2 vacancies. As mentioned previously, the case of interstitial CO_2 would deserve separate investigations. Further steps towards the elucidation of the carbonation mechanism would be related to thorough atomic-scale diffusion studies of the relevant defect species. The goal of these further works would be to reach a comparison of the efficiencies of several diffusion mechanisms for O and C within the carbonate layer. This comparison would allow to select the more efficient mechanism, which would be of direct utility in more macroscopic studies of CaO carbonation by CO_2 . in closer connection with practical issues.

CONCLUSION

The present work was devoted to a thorough atomic-scale study, by means of density functional calculations, of the point defect properties in CaCO_3 calcite. In addition to vacancies and antisite atoms, the stability of interstitials was explored by means of ab initio molecular dynamics, revealing that this possibility should be discarded for Ca and C, while interstitial O should be taken into account. The intrinsic complexity of this ternary compound

giving rise to a wide panel of point defects, we first investigated neutral defects, which conveniently provided a survey of the influence of the overall compound composition on the point defect properties. This influence appeared as rather complex, with numerous composition domains limited by various tie-lines. This demonstrated the importance of determining the conditions of composition, or equivalently chemical potentials, undergone by CaCO_3 , especially during growth. In the practically important framework of improving our knowledge of CaCO_3 formation from calcium oxide and CO_2 gas, chemical potentials were therefore determined for experimental conditions. In addition, the role of charged defects, well known in semiconductors but far less documented in carbonates, was analysed. This pointed out O and C vacancies as thermally important defects, together with interstitial O. The latter conclusion has important consequences on CO_2 diffusion within CaCO_3 and CaCO_3 growth, since it is consistent with joint C and O diffusion via vacancy mechanisms of roughly equal amplitudes. As regards the possible influence of complex point defects, our results suggest that, while interstitial diffusion of CO_2 is unfavourable, a strong binding of the CO_2 vacancy may enhance CO_2 diffusion.

List of references

- [1] Boot-Handford, M. E.; Abanades, J. C.; Anthony, E. J.; Blunt, M. J.; Brandani, S.; Mac Dowell, N.; Fernandez, J. R.; Ferrari, M. C.; Gross, R.; Hallett, J. P.; Haszeldine, R.S.; Lyngfelt, A.; Porter, R.T.J.; Pourkashanian, M.; Rochelle, G.T. Carbon capture and storage update *Energy and Environmental Science* **2014**, *7*, 130-189.
- [2] Mess, D.; Sarofim, A. F.; Longwell, J. P. Product layer diffusion during the reaction of calcium oxide with carbon dioxide. *Energy Fuels* **1999**, *13*, 999-1005.
- [3] Rouchon, L.; Favergeon, L.; Pijolat, M. New kinetic model for the rapid step of calcium oxide carbonation by carbon dioxide. *J. Therm. Anal. Cal.* **2014**, *116*, 1181-1188.
- [4] Fidler, D. K.; Gale, J. D.; Cygan, R. T. A shell model for the simulation of rhombohedral carbonate minerals and their point defects. *American Mineralogist* **2000**, *85*, 217-224.
- [5] de Leeuw, N. H.; Cooper, T.G.; Nelson, C.J.; Mkhonto, D.; Ngoepe, P.E. Computer simulation of surfaces of metals and metal-oxide materials. NATO Science Series, Series III: Computer and Systems Sciences **2003**, *187* (Computational Materials Science), 218-244.
- [6] Lardge, J.S.; Duffy, D.M.; Gillan, M.J.; Watkins, M. Ab initio simulations of the interaction between water and defects on the calcite (10 $\bar{1}$ 4) surface. *J. Phys. Chem. C*, **2010**, *114*, 2664-2668.
- [7] Rohl, A. L.; Wright, K.; Gale, J. D. Evidence from surface phonons for the (2x1) reconstruction of the (10 $\bar{1}$ 4) surface of calcite from computer simulation. *American Mineralogist* **2003**, *88*, 921-925.
- [8] Akiyama, T.; Nakamura, K.; Ito, T. Atomic and electronic structures of CaCO₃ surfaces. *Phys. Rev. B* **2011**, *84*, 085428(1-10).
- [9] Besson, R.; Favergeon, L. Atomic-scale study of calcite nucleation in calcium oxide. *J. Phys. Chem. C* **2013**, *117*, 8813-8821.

- [10] Kresse, G.; Furthmüller, J. Efficient iterative schemes for ab initio total-energy calculations using a plane-wave basis set. *Phys. Rev. B* **1996**, *54*, 11169-11186.
- [11] Kresse, G.; Furthmüller, J. Efficiency of ab initio total-energy calculations for metals and semiconductors using a plane-wave basis set. *Comput. Mater. Sci.* **1996**, *6*, 15-50.
- [12] Kresse, G.; Joubert, D. From ultrasoft pseudopotentials to the projector augmented-wave method. *Phys. Rev. B* **1999**, *59*, 1758-1775.
- [13] Perdew, J. P.; Burke, K.; Ernzerhof, M. Generalized Gradient Approximation Made Simple. *Phys. Rev. Lett.* **1996**, *77*, 3865-3868.
- [14] Besson, R. Point defects in multicomponent ordered alloys: Methodological issues and working equations. *Acta Mater.* **2010**, *58*, 379-385.
- [15] Kwon, J.; Thuinet, L.; Avettand-Fènoël, M.-N.; Legris, A.; Besson, R. Point defects and formation driving forces of complex metallic alloys: atomic-scale study of Al₄Cu₉. *Intermetallics* **2014**, *46*, 250-258.
- [16] Van de Walle, C. G.; Neugebauer, J. First-principles calculations for defects and impurities: Applications to III-nitrides. *J. Appl. Phys.* **2004**, *95*, 3851-3879.
- [17] Erhart, P.; Albe, K. Modeling the electrical conductivity in BaTiO₃ on the basis of first-principles calculations. *J. Appl. Phys.* **2008**, *104*, 044315(1-8).
- [18] Lany, S.; Zunger, A. Assessment of correction methods for the band-gap problem and for finite-size effects in supercell defect calculations: Case studies for ZnO and GaAs. *Phys. Rev. B* **2008**, *78*, 235104(1-25).
- [19] Bjerg, L.; Madsen, G. K. H.; Iversen, B. B. Ab initio calculations of intrinsic point defects in ZnSb. *Chem. Mater.* **2012**, *24*, 2111-2116.
- [20] Aberg, D.; Erhart, P.; Lordi, V. Contributions of point defects, chemical disorder, and thermal vibrations to electronic properties of Cd_{1-x}Zn_xTe alloys. *Phys. Rev. B* **2013**, *88*, 045201(1-9).

- [21] Jund, P.; Viennois, R.; Colinet, C.; Hug, G.; Fèvre, M.; Tédénac, J.-C. Lattice stability and formation energies of intrinsic defects in Mg₂Si and Mg₂Ge via first principles simulations. *J. Phys.: Condens. Matter* **2013**, *25*, 035403(1-10).
- [22] Zacherle, T.; Schmidt, P. C.; Martin, M. Ab initio calculations on the defect structure of β -Ga₂O₃. *Phys. Rev. B* **2013**, *87*, 235206(1-10).
- [23] Besson, R.; Legris, A.; Morillo, J. Comprehensive ab initio thermodynamic treatment of impurities in ordered alloys: Application to boron in B2 Fe-Al. *Phys. Rev. Lett.* **2002**, *89*, 225502(1-4). Numerical facilities for IPDA can be found at <http://adpi.univ-lille1.fr/adpi>.
- [24] Todorova, M.; Neugebauer, J. Extending the concept of defect chemistry from semiconductor physics to electrochemistry. *Phys. Rev. Applied* **2014**, *1*, 014001(1-15).
- [25] Tingaud D.; Besson, R. Point defects and diffusion in ordered alloys : an ab initio study of the effect of vibrations. *Intermetallics* **2014**, *45*, 38-45.
- [26] Besson, R.; Rocha Vargas, M.; Favergeon, L. CO₂ Adsorption on Calcium Oxide: An Atomic-Scale Simulation Study. *Surface Science* **2012**, *606*, 490-195.
- [27] Rouchon, L.; Favergeon, L.; Pijolat, M. Analysis of the kinetic slowing down during carbonation of CaO by CO₂. *J. Therm. Anal. Cal.* **2013**, *113*, 1145-1155.
- [28] Nikulshina, V.; Galvez, M. E.; Steinfeld, A. Kinetic analysis of the carbonation reactions for the capture of CO₂ from air via the Ca(OH)₂-CaCO₃-CaO solar thermochemical cycle. *Chem. Eng. J.* **2007**, *129*, 75-83.

